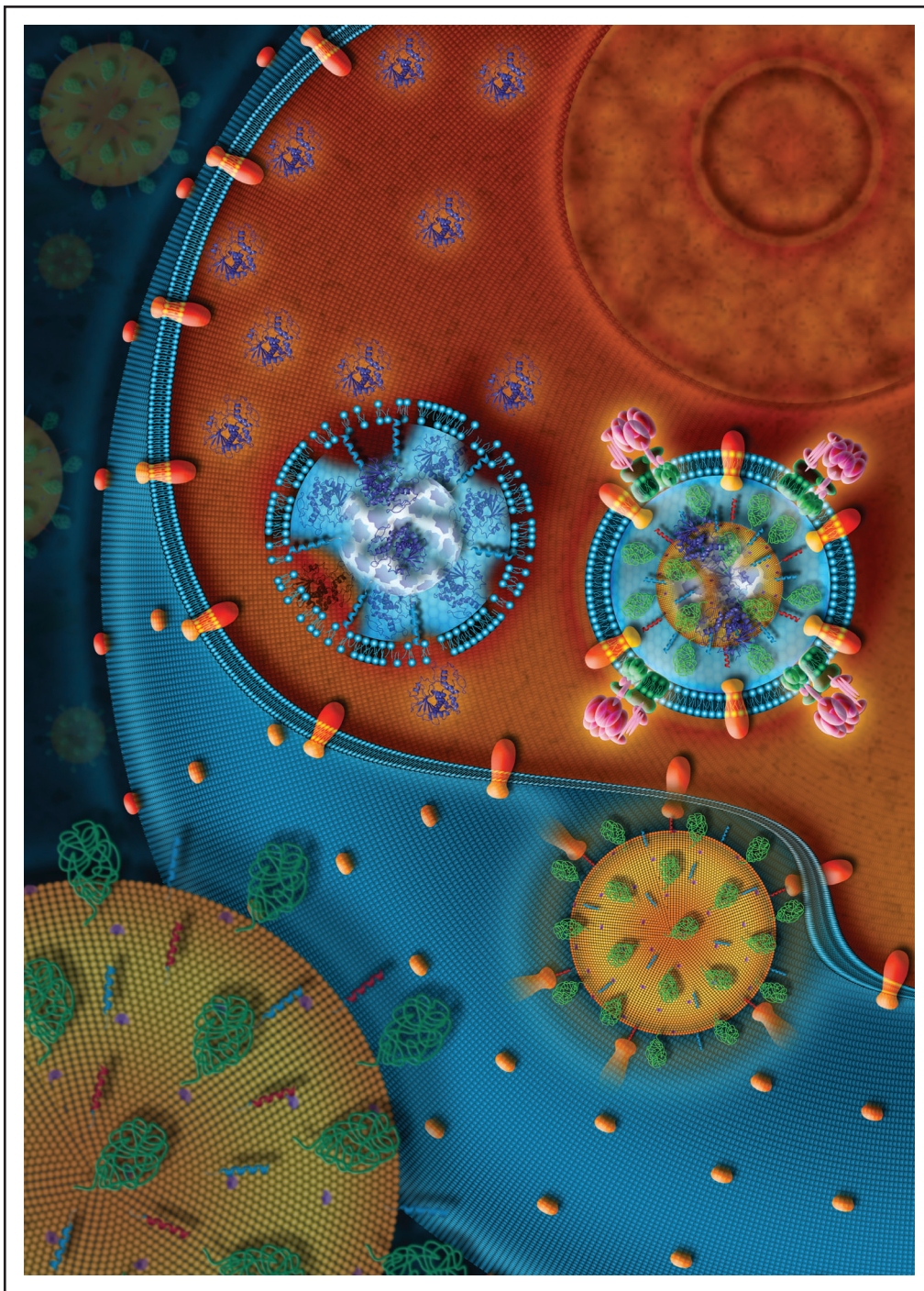


# ADVANCED HEALTHCARE MATERIALS



# Small-Diameter Silk Vascular Grafts (3 mm Diameter) with a Double-Raschel Knitted Silk Tube Coated with Silk Fibroin Sponge

Derya Aytemiz, Wataru Sakiyama, Yu Suzuki, Naoki Nakaizumi, Ryou Tanaka, Yoko Ogawa, Yoshihide Takagi, Yasumoto Nakazawa, and Tetsuo Asakura\*

Small-diameter (less than 6 mm in diameter) vascular grafts are highly desirable due to the large demand for surgical revascularization; however, there are no available artificial grafts. Vascular grafts of 1.5 mm diameter prepared by our group with silk fibroin fiber have been proved to be excellent grafts with remarkably high patency and remodeling, based on rat implantation experiment (Enomoto et al., 2010). In this study, a silk fibroin vascular graft with 3 mm diameter which can be used for the coronary arteries or lower extremity arteries is prepared with a double-raschel knitted *Bombyx mori* silk fiber tube coated with *B. mori* silk fibroin sponge. Here the silk sponge is prepared from an aqueous solution of the silk fibroin and poly(ethylene) glycol diglycidyl ether as porogen. Sufficient strength, proper elasticity, and protection from loose ends in the implantation process are obtained for the silk fibroin graft; low water permeability and relatively large compliance are also attained. These excellent physical properties make silk fibroin grafts suitable to be implanted in a canine model.

## 1. Introduction

Artificial grafts are becoming more desirable with the increasing number of patients requiring replacement of their coronary and lower extremity arteries. Accordingly, many researchers have long attempted to develop artificial grafts. Synthetic vessels such as poly(tetrafluoroethylene) (e-PTFE) and knitted or woven poly(ethylene terephthalate) (PET) grafts (Dacron) are commercially available and have performed satisfactorily for

grafts larger than 6 mm in internal diameter (ID).<sup>[1]</sup> Specifically, the patencies of e-PTFE and Dacron grafts (6 mm ID) were 26–46% and 42–62%, respectively, at 5 years follow-up time.<sup>[2]</sup> However, grafts with smaller than 6 mm ID fail early due to thrombus formations and intimal hyperplasia.<sup>[3,4]</sup> Animal studies have shown only a 20–25% patency rate with 1 mm diameter PTFE grafts, while all vein grafts in a similar size remained patent.<sup>[5,6]</sup>

Silk fibroin (SF) fiber from *Bombyx mori* has a long history of use in textiles. SF fiber also has a long history of use as a suture material because of its high strength and toughness.<sup>[7]</sup> Moreover, SF has been reported to have many inherent superior properties as a biomaterial in terms of mechanical properties, environmental stability, biocompatibility, low immunogenicity, and biodegradability.<sup>[8–11]</sup>

therefore, many applications of SF biomaterials have been examined.<sup>[12–16]</sup> SF has been previously studied as biomaterial substrates for cell growth related to tissue engineering. Electrospun and porous silk composite scaffolds have been used for ingrowth of human mesenchymal stem cells (hMSCs) to osteogenic tissue formation in vitro. Both scaffolds supported high calcium deposition and cell differentiation.<sup>[16–19]</sup>

In our previous studies,<sup>[20,21]</sup> we prepared SF grafts by braiding, flattening, and winding the SF fibers onto a cylindrical polymer tube followed by coating with an SF aqueous solution. The grafts, which are 1.5 mm in ID and 10 mm in length, were implanted into rat abdominal aorta. An excellent patency (85.1%;  $n = 27$ ) at 1 year after grafting with SF fibers was obtained. This patency rate was remarkably higher than that of e-PTFE grafts (30%;  $n = 10$ ,  $p < 0.01$ ). Endothelial cells and smooth muscle cells were organized early on the inner layer of the SF graft. Sirius-red staining revealed that the collagen content of fibroin grafts significantly increased 1 year after implantation, with a decrease in SF content.<sup>[20]</sup> However, this graft has some problems when used with larger diameter (3 mm) for the coronary arteries or lower extremity arteries because of its relatively weak strength, lack of elasticity, and tendency for the end of the graft to become loose during the implantation process, which are not very serious problems in

D. Aytemiz, W. Sakiyama, Dr. Y. Suzuki, Dr. Y. Nakazawa, Prof. T. Asakura  
Division of Biotechnology and Life Science  
Tokyo University of Agriculture and Technology  
Koganei, Tokyo 184-8588, Japan  
E-mail: asakura@cc.tuat.ac.jp

N. Nakaizumi, Dr. R. Tanaka  
Division of Animal Life Science  
Tokyo University of Agriculture and Technology  
Fuchu, Tokyo 183-8509, Japan

Y. Ogawa, Y. Takagi  
Fukui Wrap Knitting Co., Ltd, 3-519-3 Nishikaihatsu  
Fukui, Fukui 910-8512, Japan



DOI: 10.1002/adhm.201200227

rat implantation experiment; however, they become more serious problems in implantation for larger animals.

In this study, we report SF grafts prepared as a double-raschel knitted SF fiber graft that is coated with SF aqueous solution containing poly(ethylene) glycol diglycidyl ether (PGDE) in order to overcome these problems. We have already shown that SF grafts prepared by this method could avoid early formation of thrombosis until 8 weeks after implantation in rat abdominal aorta.<sup>[21]</sup> Following the rat study, SF vascular grafts with small diameter (3 mm) were fabricated using a double-raschel knitting technique, which is especially useful for preparation of larger-diameter SF grafts because of its sufficient strength, proper elasticity, and protection from formation of loose ends during the implantation process. In addition, coating of the grafts with a mixture of SF aqueous solution and PGDE was used in order to construct porous structures of SF on the graft surface; here, PGDE is used as porogen. SF vascular graft was then used in a practical application for a dog study. We performed bilateral end-to-end common carotid arteries (CCA) bypasses with 3 mm diameter SF grafts in a canine model, and the graft patency and hemodynamic changes were monitored with color Doppler ultrasonography.

## 2. Results and Discussion

### 2.1. Preparation of SF Grafts

As summarized in **Figure 1** for a single-coated SF graft, SF grafts with 3 mm inner diameter were prepared carefully. An SEM image of the double-raschel knitted SF grafts with 3 mm inner diameter after degumming treatment are shown in **Figure 2A**. The remaining silk sericin in the knitting process was removed completely. The double-raschel knitting has merit

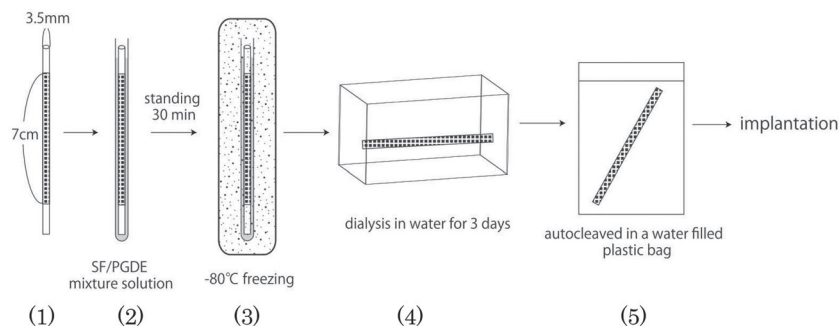


**Figure 1.** Preparation process of a single-coated SF graft: 1) a 3 mm AC rod was covered by double-raschel knitted SF tube, 2) the rod with SF tube was inserted in AC pipe with 5 mm inner diameter and the space was filled with mixed SF/PGDE aqueous solution, 3) the graft was frozen at  $-80^{\circ}\text{C}$  for 24 h in a refrigerator, 4) the graft was allowed to stand in deionized water for 3 d, and, 5) the graft was placed in a bag and sterilized using an autoclave at  $120^{\circ}\text{C}$  for 20 min.

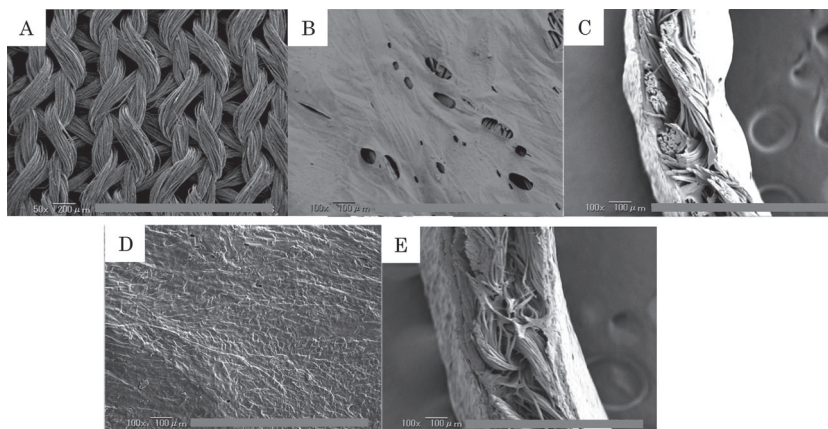


**Figure 2.** SEM images of several SF grafts: A) the surface of a double-raschel knitted silk fiber tube after removal of silk sericin, B) inner surface of the single-coated graft, C) cross-section of the single-coated graft, D) inner surface of the double-coated graft, and, E) cross-section of the double-coated graft. The thicknesses of the grafts were: C)  $300\ \mu\text{m}$ , and, E)  $500\ \mu\text{m}$ .

in that the silk threads do not become flat even if the threads are pressurized by a guide or needle, as well as having appropriate elasticity. In addition, because of many contact points of the fibers, sufficient strength and protection from loosening at the edges in the implantation process could be attained. The friction on the contact point was also reduced, which prevents thread tears and/or thread separation during manufacturing process.

The SF graft was coated with SF sponge using PGDE as porogen to decrease the leakage of blood from the graft, to protect from the loosening of the fibers at the edges in the implantation process, and to strengthen the elastic character of the graft. Min et al.<sup>[22]</sup> prepared porous tubular scaffolds from only SF aqueous solution with the addition of PGDE. The scaffolds were flexible and transparent in the wet state with a pore size of  $81\text{--}128\ \mu\text{m}$  and porosity of 90% to 96%, depending on the concentrations of SF and PGDE. The tubular SF scaffolds had satisfying tensile and compression properties, especially an excellent deformation-recovery ability. No obvious cytotoxicity to mouse L-929 fibroblasts was detected. Thus, this SF/PGDE sponge coating on the degummed double-raschel knitted SF graft was performed at the steps 2–4 in **Figure 1**. The PGDE was removed completely at step 4. PGDE has usually been used as cross-linking agent via heat treatment. However, in our experiment, this reagent is used as porogen and there are no cross-linking between silk fibroin and PGDE because there is no heat treatment, see **Figure 1**. **Figures 2B** and **C** show SEM pictures of the inner surface and cross-section of the single-coating graft with 5% SF concentration and SF/PGDE of 1:1. The thickness of the graft was  $300\ \mu\text{m}$ . At the surface, there are holes,  $50\text{--}200\ \mu\text{m}$  randomly. Double coating with 5% SF concentration and SF/PGDE of 1:1 leads to the formation of an inner surface with essentially no holes, as shown in **Figure 2D**; the thickness was  $500\ \mu\text{m}$  (**Figure 2E**).

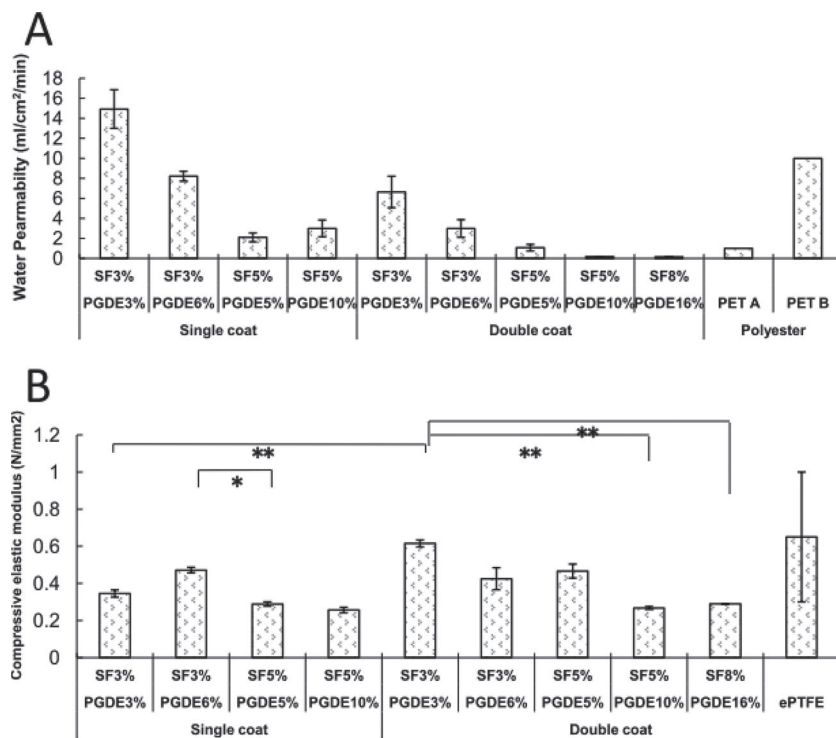


**Figure 3.** A) Water permeabilities of several SF grafts: single-coated with SF 3% and SF/PEGD of 1:1 and 1:2; with and SF 5% and SF/PGDE of 1:1 and 1:2; and double-coated with SF 3% and SF/PEGD of 1:1 and 1:2, with SF 5% and SF/PGDE of 1:1 and 1:2, and with SF 8% and SF/PEGD of 1:2; also shown are PET A (Triprex, Terumo, Japan) and PET B (J Graft sealed, Junken Medical, Japan).<sup>[23]</sup> The statistical errors were determined using one-way analysis of variance (ANOVA) and Tukey-Kramer post hoc tests, \* $P < 0.05$ , \*\* $P < 0.001$ ; error bars indicate  $\pm$ SD;  $n = 5$ . B) Corresponding compressive elastic modulus of several SF grafts, together with that of ePTFE.<sup>[21]</sup> The statistical errors were determined using one-way analysis of variance (ANOVA) and Tukey-Kramer post hoc tests, \* $P < 0.05$ , \*\* $P < 0.001$ ;  $\pm$ SD;  $n = 7$ .

## 2.2. Physical Properties

The physical properties were measured for the SF grafts prepared by single- or double-coating, at different SF concentrations and ratios of SF/PGDE.

The water permeabilities of the SF grafts are plotted against the SF concentration and the ratio of SF/PGDE as shown in Figure 3A together with two corresponding values reported in the specification of the two commercial sealed-polyester vascular prostheses, PET A (Triprex, Terumo, Japan) and PET B (J Graft sealed, Junken Medical, Japan).<sup>[23]</sup> The water permeability decreases for the double-coated graft compared with the single-coated one, as is expected from Figure 2. In addition, with increasing SF concentration or the fraction of PGDE in the graft preparation process, the water permeability tends to decrease. The water permeability of the double-coated grafts with 5% SF concentration with SF/PGDE of 1:2 or with 8% SF concentration with SF/PGDE of 1:2 were  $0.17 \pm 0.02$  mL and  $0.13 \pm 0.02$  mL (\* $p < 0.05$ ), respectively. These values are smaller than the PET A, indicating sufficient coating is achieved by SF sponge on the SF tube.

Next, the compressive elastic modulus was observed; the results are summarized in Figure 3B. The modulus tends to

decrease with increasing SF concentration and with fraction of PGDE. The double-coated grafts also tend to have higher compressive elastic modulus than those of single-coated grafts. However, the difference between single- and double-coated grafts becomes small for the grafts with 5% SF concentration and SF/PGDE of 1:2. These compressive elastic modulus values are lower than that of ePTFE.<sup>[21,24]</sup> Thus, SF grafts with 5% SF concentration and SF/PGDE of 1:2 seem to be favorable for artificial grafts from the viewpoint of compressive elastic moduli, as well as having the very low water permeability mentioned above. When we mixed SF aqueous solution with PGDE, structural transition of the SF from random coil to  $\beta$ -sheet structure occurs. However, the ability of PGDE to form  $\beta$ -sheet structure of SF molecules is not so strong, for example, compared with polar solvents such as methanol or acetone. After removal of PGDE, an SF sponge coating on the double-raschel knitted SF fiber graft with suitable character for the artificial vascular graft was attained.

## 2.3. Acute Thrombogenicity

Clot weight gain was evaluated by acute thrombosis determination with in vitro pig blood circuit methods. Vascular patency relies on a careful balance of chemical mediators and local fluid dynamics.<sup>[23]</sup> Blood flow through vascular grafts is believed to correspond with thrombosis formation. In this study, we attempted to simulate a blood circuit. Measurement of clot weight corresponds to platelet and fibrin deposits and red blood cell adhesion on the SF graft surfaces. The results are summarized in Figure 4. It can be pointed out that non-coated and single-coated grafts clearly show higher weight increase compared with the double-coated one, by more than a factor of two (\* $p < 0.05$ , \*\* $p < 0.001$ ). This result is related to the roughness of the surfaces, as shown in Figure 2A; that is, higher roughness of the former grafts. The concern was whether fresh blood would deteriorate gradually during circulation. Blood components, such as erythrocytes, leukocytes, thrombocytes, and hemoglobin, were within normal ranges for 90 min during circulation (data not shown). The inner circuit pressure was between 75 and 115 mmHg. Indeed, it was concluded that using the circuit would demonstrate conditions mimicking in vivo dynamic blood flow to some extent for 90 min of experiment. Thus, the double-coated graft seems favorable, although there are no significant differences with changing SF concentration or ratio of SF/PGDE. This multifunctional vascular prosthesis has not only outstanding mechanical properties and porous structure, but also hemocompatibility, which is an important characteristic for preventing acute thrombosis and facilitating the tissue development.

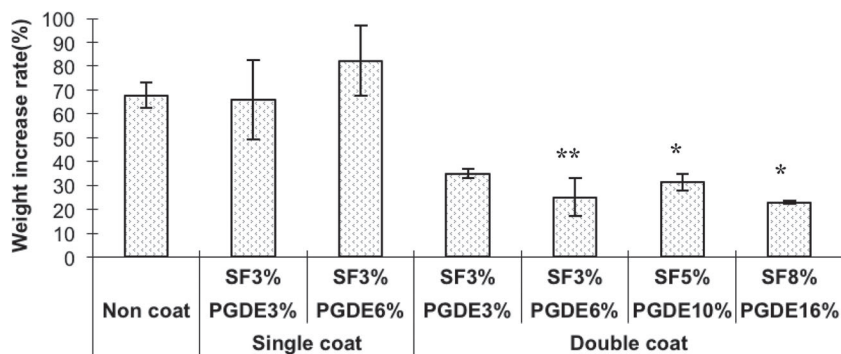


**Figure 4.** Weight increase percentage (%) rate of SF grafts. Non-coated; single-coated with SF 3% and SF/PEGD of 1:1 and 1:2, and with SF 5% and SF/PGDE of 1:1 and 1:2; and double-coated with SF 3% and SF/PEGD of 1:1 and 1:2, with SF 5% and SF/PGDE of 1:1 and 1:2, and with SF 8% and SF/PEGD of 1:2. The statistical errors were determined using one-way analysis of variance (ANOVA) and Tukey-Kramer post hoc tests, \* $P < 0.05$ , \*\* $P < 0.001$ ; errors bars indicate  $\pm$ SD;  $n = 7$ ).

## 2.4. Compliance

Judging from the water permeability, compressive elastic modulus, and acute thrombogenicity experiments, we selected the double-coated SF grafts with 5% SF concentration and SF/PGDE of 1:2 for evaluation of the SF graft using a canine model.

Previous studies demonstrated that the patency is significantly correlated with compliance when synthetic vessel grafts were implanted in animal models.<sup>[25,26]</sup> Thus, before dog implantation experiments, the compliance of the graft (5% SF concentrations and SF/PGDE of 1:2) was determined. The intra-luminal pressure ( $P$ )–relative diameter ( $D$ ) curves of the double-coated SF grafts and ePTFE grafts used as a control are shown in **Figure 5**. The  $P$ – $D$  curve of the SF graft was a typical J-type pattern. This pattern is the same as that of native artery, although the compliance, 1.90, of the SF graft at 100 mmHg is smaller than the value 6.8 of native artery at 100 mmHg (**Table 1**).<sup>[26]</sup> In contrast, the ePTFE grafts showed only small change in the diameter during the experiment, which was quite a different pattern to the SF grafts. The value,

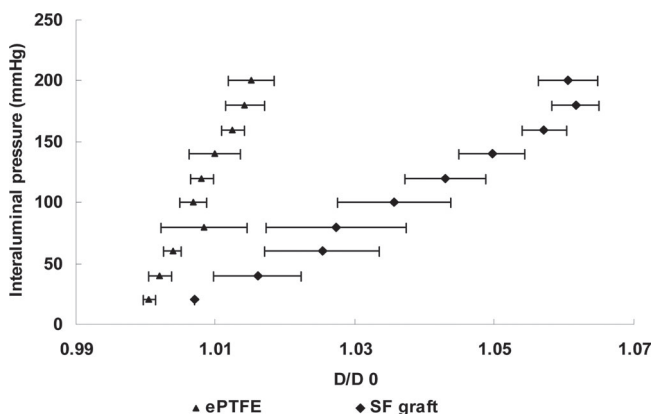


**Figure 5.** Compliance experiment. The intraluminal pressure was plotted against external diameter relative to the original diameter  $D_0$  at no pressure for ePTFE ( $\blacktriangle$ ) and SF ( $\blacklozenge$ ) grafts. The standard deviations are shown with error bars.

0.51, at 100 mmHg is quite small compared with native artery. Thus, the SF graft is suitable to the artificial graft from the viewpoint of compliance. The  $\beta$ -value of the SF graft is 24.84, which is close to the value of native artery, 10.6.<sup>[26]</sup> Thus, it is concluded that the SF graft is favorable for the artificial graft.

## 2.5. Implantation and Color Doppler Sonography

The post-operative course for each dog was uncomplicated. No late neurological complications were observed. All SF grafts used here were patent after operation, no intraoperative acute thrombosis was observed. **Figure 6A** shows an SF graft after implantation; blood oozing and good matching with the native artery can clearly be observed. The character of the implanted graft Doppler velocity waveform is shown in **Figure 6B**. Intimal hyperplasia and acute thrombosis following arterial bypass grafting with small-diameter prosthetic material often results in treatment failure. Therefore, it is critical to study this problem and important to have animal models. In this study, we applied the SF graft with the ratio values of 5% SF and 10% PGDE to a canine carotid artery bypass graft model. After implantation, the performance of the graft was evaluated by color Doppler sonography for the acute thrombosis and blood hemodynamics.

Of five implanted grafts, four were observed over four weeks and one graft was observed over one year. For the one-year observations, vascular graft sonography monitorization was carried out post-operatively 1 month, 6 months, and every 2 months to 1 year to observe hemodynamic and intimal changes. Four-months post-operatively the grafts showed regular enhancement without perfusion defects. This event may be proof of the graft remodeling and gaining strength in vivo. Hemodynamic changes of peak systolic velocity (PSV; **Figure 7A**) and end diastolic velocity (EDV; **Figure 7B**) were observed for one year. One-month post-operatively, PSV increased in the middle portion of the vascular prosthesis; however, the EDV increase was not significant. Six months after operation, PSV increases were still observed in the middle portion of the vascular prosthesis, with an increase in EDV also observed. Eight months after operation, the PSV and EDV increases shifted from the middle portion to a proximal anastomosis portion. Detection of a hemodynamically significant focal increase in PSV means that there may be formation of stenosis in the segment where the

**Table 1.** Diameter compliance and stiffness of grafts (ePTFE and SF graft).

	Compliance [% per 100 mmHg]	$\beta$
SF Graft	1.90	24.84
ePTFE	0.51	164.00
Native artery*	6.80	10.60

\*These values were taken from Sonoda et al.<sup>[26]</sup>

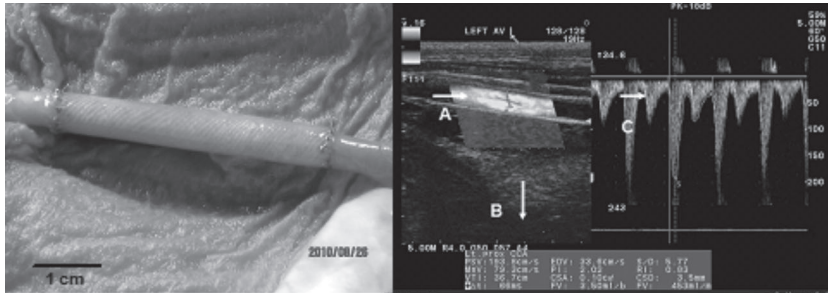


**Figure 6.** A) SF graft after implantation; blood oozing and good matching with native artery can be observed. B) Doppler velocity waveform of implanted SF graft. A: direction of blood flow, B: depth on the B mode, C: time axis on the pulse Doppler mode.

increase in PSV was detected. This result may suggest initial plaque or stenosis formation in the middle portion of vascular prosthesis in the first six months and proximal anastomosis portion in the second six months.

## 2.6. Histological Analysis

One-month and one-year post-operatively hematoxylin & eosin (H&E) and Masson's trichrome staining were analyzed. After

one month, H&E staining showed fibrin and blood-cell immigration into the vascular graft and the remaining coating material (Figure 8A). SF vascular grafts did not show any necrosis or calcification. Histological analysis one month after grafts implantation is too early to observe neovessel formation and inflammatory cell response for degradation. There were no fibrous tissue formations on the graft wall (Figure 8B and C). One year after implantation the medial portion of the graft showed inflammatory cell infiltration throughout the SF graft, including macrophages, neutrophils, lymphocytes, and plasma cells. After one year, the SF sponge was almost degraded and replaced by fibrous tissue (Figure 8E and F). Such fibrous tissue is the biggest part of the native artery of collagen observed by Masson's trichrome on the graft wall. Endothelial and smooth muscle-like cell were observed on the luminal area for proximal and distal parts of vascular grafts by H&E staining (Figure 8D). However the middle portion of SF graft did not show endothelial cell formation. Long-term graft failure of polyester substrate are due to calcification or graft infection following necrosis in current use. After one year, SF did not show any necrosis, calcification or infection formation. In addition, change of the SF graft wall to fibrous native tissue was observed. Acute inflammatory cells, but not giant inflammatory cells, were also observed. This result suggests that SF shows a low body immune response with degradation.

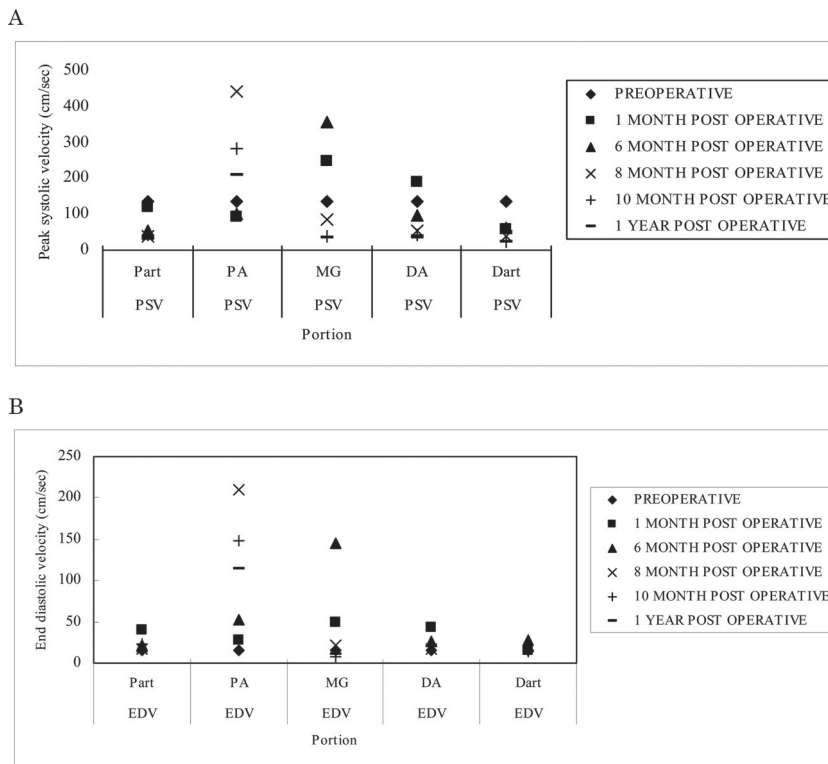


**Figure 7.** Peak systolic velocity (PSV) and end diastolic velocity (EDV) values of implanted SF graft from the dog one year after implantation. In the first six months, PSV and EDV slightly increased in the mid-portion of the vascular graft; however, in the second six months increases in PSV and EDV have shifted in proximal anastomosis portion. Increased PSV and EDV values indicated stenosis formation in proximal part of implanted graft. The labels indicate: Part: proximal native artery, PA: proximal anastomosis, MG: middle part of vascular graft, DA: distal anastomosis, and, Dart: Distal native artery.

## 3. Conclusions

This study proposed a novel technique to fabricate small-diameter vascular grafts assembled from knitted SF tube and SF coating which can be used for the coronary arteries or lower extremity arteries. The grafts exhibited a good scaffold with desirable mechanical properties essential to increased efficacy for revascularization and handling during surgical operation. Moreover, we demonstrated that properties such as permeability can be controlled by a concentration of SF-mixed PGDE to solidify SF solution and to provide elastic characteristics. In addition, a higher concentration SF solution showed higher elastic modulus. A double-coated method showed better compliance under hydrostatic pressure. In conclusion, the double-coated graft with 5% SF and 10% PGDE was the most functional one observed in this study. This graft was used to perform bilateral end-to-end CCA bypasses in a dog study and one of the implanted grafts showed patency more than one year after implantation. These results suggest the potential of the SF

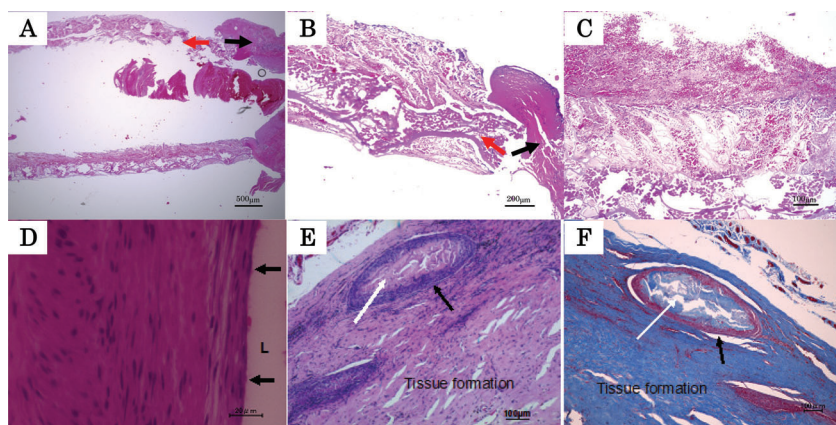


**Figure 8.** A) Silk fibroin graft one month after implantation with hematoxylin and eosin (HE) staining at proximal anastomosis. The black arrow shows the native vessel of the dog and the red arrow shows the silk fibroin graft. Fibrin and blood-cell immigration into the vascular graft was observed and the coating material of the graft remained intact. B) Higher magnification of proximal anastomosis. The black arrow indicates the native vessel of the dog and the red arrow the silk fibroin graft. The silk fibroin graft shows cell immigration into the vascular wall and the coating material. C) Higher magnification of (B); cell attachment is observed on the coating material. D) Silk fibroin graft one year after implantation: HE staining shows an endothelial cell layer and smooth muscle-like cell inner parts of lumen, (L: lumen). E) Higher magnification of HE staining. Silk fibroin substrata among inflammatory cells are observed. No giant cell is observed. F) MTC staining of the silk fibroin graft one year after implantation. In the silk fibroin substrate, inflammatory cell and tissue formation composed of collagen are observed. These findings shows the inflammation process is still ongoing.

graft to regenerate vasculatures. The results encourage further studies on SF knitted grafts coated with SF/PGDE for vascular applications.

## 4. Experimental Study

### 4.1. Preparation of the Double-Raschel Knitted SF Tube

A computer-controlled double-raschel knitting machine was used to prepare knitted SF tubes with 3 mm ID. The machine is usually used to prepare graft tubes with polyester fiber with sufficient strength and long filaments. To prepare double-raschel SF tubes, firstly, SF thread from *B. mori* was degummed in such a way that some part of silk sericin could remain to avoid breaking of SF thread in the knitting process. Then the SF threads obtained were tied up in a bundle and knitted to manufacture double-raschel knitted SF tube. For the knitting process, several degummed SF fibers were braided together and the braided SF was used for preparing the tubular graft with the double-raschel knitting method. The double-raschel knitted SF tubes were then degummed in a mixture of sodium carbonate (0.08% w/v) and Marseille soap (0.12% w/v) solution at 95 °C for 120 min in order to remove the silk sericin completely before coating with SF aqueous solution.

### 4.2. Preparation of SF Aqueous Solution for Coating

For coating double-raschel knitted SF tubes, *B. mori* SF aqueous solution was prepared. The dried silk threads were degummed

in order to remove silk sericin, as described above. The degummed SF fibers were dissolved in a 9 M lithium bromide solution to a concentration of 20% (w/v) at 60 °C for 4 h and then dialyzed against distilled water for 3 d at 4 °C using a cellulose membrane (MWCO 14 000). The final concentration of the fibroin aqueous solution was 3%–8% (w/v). Freshly prepared SF aqueous solution was subsequently used for coating the SF graft.

### 4.3. Preparation of the SF Graft by Coating with SF Sponge

We tried two coating methods, single and double coating. Figure 1 summarizes the process used to prepare SF grafts, with single coating as an example. The acrylic (AC) rod with 3 mm diameter was covered by double-raschel knitted SF tube with 3 mm inner diameter (Step 1). The rod covered by the silk tube was inserted in an AC pipe with 5 mm inner diameter, where the bottom was sealed by a paraffin film, and the space between the rod and pipe was filled with the mixed SF/PGDE aqueous solution (Step 2) and the graft was frozen immediately at –80 °C for 24 h (Step 3); the concentration of silk fibroin was changed, 3% or 5%, and the composition of SF/PGDE solution was changed, SF/PGDE of 1:1 or 1:2. Then the silk tube was pulled out from the rod and put in deionized water for 3 d (Step 4), where the water was replenished twice daily. The graft was put in a bag and sterilized using an autoclave at 120 °C for 20 min (Step 5).

The double-coated SF graft was prepared after the single-coating process. An SF tube with slightly larger inner diameter (4 mm diameter instead of 3 mm diameter) was used at the first coating. Then, 3 mm diameter AC rod was inserted into the single-coated tube with 4 mm inner diameter carefully. The space between the rod and silk tube was filled with the mixed SF/PGDE aqueous solution and the graft was frozen immediately at –80 °C for 24 h. The concentration of silk fibroin was changed, to be 3%, 5% or 8%, and the composition of SF/PGDE solution was changed, with SF/PGDE of 1:1 or 1:2. The removal of PGDE was confirmed by no detection of PGDE peaks in the IR and NMR spectra of the graft (Data not shown).

### 4.4. Physical Property Observations

The complete removal of PGDE from the SF graft was confirmed with FT-IR (JASCO FT/IR 4100, Japan) and <sup>13</sup>C CP/MAS NMR (JEOL 400 MHz NMR spectrometer, Japan) spectroscopies. A scanning electron microscopy (SEM; VE-7800 Keyence, Japan) was used to check the morphology of the SF graft.

The water permeability test was carried out according to ISO7198 in order to evaluate blood leakage of SF grafts. A water

reservoir was connected to a polyethylene tube followed by the graft and then an amount of 120 mmHg hydrostatic pressure was applied to the graft. The permeated water through the graft wall per minute was collected and calculated in  $\text{ml min}^{-1} \text{cm}^{-2}$ . For the longitudinal suture retention test, the sample tube was cut to 15 mm length and then the segment was cut to a 15 mm  $\times$  5 mm rectangular. The edge of the test specimen was held by a clamp and the other was hooked by a loop of nylon suture (8–0 size) at 2 mm from the edge. The nylon loop was held and pulled by the clamp. The circumferential compressive elastic modulus and longitudinal suture retention were tested with tensile testing machine EZ graph (Shimadzu, Japan) in order to evaluate graft compliant and strength. For each test, a stress–strain curve was drawn using the image analysis software installed on the computer. For the circumferential compressive elastic modulus, the SF graft was cut into a known length greater than 10 mm and the outer diameter (OD) was measured before testing. The sample was hydrated with a saline solution for 1 h. This process is necessary to improve handling during implantation. The linear tensile modulus was defined by the slope of the stress–strain curve between 25% and 75% of the peak failure stress.

#### 4.5. Compliance Observation

Compliance is an especially important property for artificial graft. This was tested here using segments (3–4 cm in length) of tubes with diameter 3 mm. The SF grafts were connected to the polyvinyl tubes with a silk suture and a Teflon tape. The syringe pump was connected to the other side of a polyvinyl tube. The intra luminal pressure,  $P$ , was generated by pressurizing water and measured with a pressure transducer (Keyence AP-13S, Japan). With increasing pressure, change in the external diameter at the center of the tube,  $D$ , was observed using CCD camera (Vixen C10-4M, Japan). The pressures were plotted against the ratio of the  $D$ /original diameter ( $D_0$ ) for ePTFE and SF grafts.

The diameter compliance percentage of the tube was determined with the stiffness parameter ( $\beta$ ) defined by Hayashi et al.<sup>[25]</sup> according to the following equation:

$$\ln(P/P_s) = \beta(D/D_s - 1) \quad (1)$$

where  $P$ ,  $P_s$ ,  $D$ , and  $D_s$  denote the intra-luminal pressure, the standard pressure (100 mmHg in this study), the external diameter, and the diameter at  $P_s$ , respectively. The logarithm of the normalized pressure,  $\ln(P/P_s)$ , was plotted as a function of the normalized external diameter,  $D/D_s$ . The  $\beta$ -value was determined as the approximate slope of the plot in the physiologic blood pressure range (80–120 mmHg). The diameter compliance ( $Cd$ ) was calculated using the following equation:

$$\% Cd = (D_{120} - D_{80}) / (D_{80}(P_{120} - P_{80}) \times 104) \quad (2)$$

#### 4.6. Acute Thrombogenicity

Clot weight gain was evaluated by acute thrombosis determination with in vitro pig blood circuit methods. In each

experiment, fresh blood from the same pig was divided into separate reservoirs of 1 L. The blood was supplemented with 4 U  $\text{mL}^{-1}$  heparin (Wako, Japan). The weight of the grafts (5 cm in length) was recorded before testing. Four samples used for each concentration and samples were placed in parallel under the blood circuit. The pulsatile blood flow was provided by a peristaltic pump (Gilson, USA). The peristaltic pump was run at a flow rate 220  $\text{mL min}^{-1}$  for 90 min. The blood from the circuit was collected every 15 min to evaluate the blood components. At the end of experiment, samples were washed with 50 mL PBS under circulation for 5 min. The samples were fixed in methanol and dehydrated in ethanol at graduated concentrations. The clot weight gain was determined by subtracting the pre-testing graft weight from the post-testing weight.

#### 4.7. Implantation Methods

We used five Beagle dogs weighing between 8 and 12 kg. Before performing the implantation, the health of dogs was evaluated by general clinic examination, with blood and serum biochemical examination. Activated clotting time (ACT), activated partial thromboplastin time (APTT), prothrombin time (PT), fibrinogen concentration were measured with blood coagulation analysis equipment (Wako COAG2V, Japan). Dogs were premedicated with meloxicam (0.2  $\text{mg kg}^{-1}$  SC), atropine sulfate (0.04  $\text{mg kg}^{-1}$  SC), butorphanol tartrate (0.2  $\text{mg kg}^{-1}$  IV) and midazolam hydrochloride (0.2  $\text{mg kg}^{-1}$  IV). Induction was achieved with propofol (4  $\text{mg kg}^{-1}$  IV) after intubation. General anesthesia was maintained with inhalation of isoflurane mixed with oxygen. Through midline neck incision, both right and left common carotid arteries (CCA) were exposed. Following heparin (100 U  $\text{kg}^{-1}$  IV Ajinomoto, Japan) administration, CCA was occluded with non-crushing vascular clamps. A 2 cm length native vessel was expanded and the double-coated SF graft (SF 5%, SF/PGDE of 1:2) with 3 mm inner diameter and 3 cm length was implanted with end-to-end bypass ( $n = 5$ ). 7–0 polypropylene (Premio Peters surgical, Bobigny, France) and 10–12 interrupted stitch were used for each end of bypass. During the operation, ACT was measured every 20 min to protect acute injury thrombosis because a minimal ACT of 480 s was required before onset of bypass surgery. After implantation of both bypass grafts was completed and meticulous hemostasis was achieved, the incision was closed in two layers using an absorbable suture. Low-molecular heparin (Ajinomoto, Japan) and aspirin were administrated as anticoagulant and antiplatelet treatment after implantation.

During all phases of the present study, dogs were managed and cared for in accordance with the standards established by the Tokyo University of Agriculture and Technology (TUAT), which is described in its “Guide for the care and use of laboratory animals.” This study was approved by the animal experimental committee of TUAT, with an acceptance number of 23–79.

#### 4.8. Color Doppler Sonography

Pre- and post-operative color doppler sonography was performed on all of the dogs on common carotid artery. A color ultrasound



(Hitachi-Aloka Medical, Ltd., Pro Sound SSD- $\alpha$ 10, Japan) with 7.5 MHz linear transducer was used to monitor CCA to determine acute thrombosis and hemodynamic changes, including peak systolic velocity (PSV), end-diastolic velocity (EDV), pulse index (PI), and resistance index (RI). A minimum dose of propofol was used for sedation during color doppler sonography evaluation. Data were obtained at 5 portions, the proximal CCA (Part), proximal anastomosis (PA), mid-graft (MG), distal anastomosis (DA), and distal CCA (Dart).

#### 4.9. Histological Analysis

After fixating, vascular grafts were dehydrated in alcohol solutions of increasing concentration, clarified in xylene and embedded in paraffin. Embedded samples were cut 5  $\mu$ m using a microtome and sections were stained with hematoxylin & eosin and Masson's trichrome. The histological slides were observed under an optical microscope (Keyence, Japan). The rate of local tolerance was analyzed concerning presence of fibrous tissue, fibrin, degenerative phenomena, necrosis, neovessels, calcification, inflammatory cells, and material degradation of SF graft.

#### 4.10. Statistical Analysis

Results of physical property tests were evaluated by one-way analysis of variance (ANOVA), followed by Tukey-Kramer post hoc tests to evaluate the statistical differences among all samples. All error bars are standard error ( $\pm$ SD). Values of  $P < 0.05$  were considered significant.

#### Acknowledgements

T.A. acknowledges the support of a grant from the Ministry of Agriculture, Forestry, and Fisheries of Japan (Agri-Health Translational Research Project 2010–2015).

Received: July 6, 2012

Published online: September 27, 2012

- [1] E. C. Demiri, S. L. Iordanidis, C. F. Mantinaos, *Handchir. Mikrochir. Plast. Chir.* **1999**, *31*, 102.
- [2] R. J. van Det, B. H. R. Vriens, J. van der Palen, R. H. Geelkerken, *Eur. J. Endovasc. Surg.* **2009**, *37*, 457.
- [3] J. S. Budd, K. E. Allen, G. Hartley G, P. R. Bell, *Eur. J. Vasc. Surg.* **1991**, *5*, 397.
- [4] B. L. Seal, T. C. Otero, A. Panitch, *Mater. Sci. Eng. R* **2001**, *34*, 147.
- [5] R. H. Schmedlen, W. M. Elbjairami, A. S. Gobin, J. L. West, *Clin. Plast. Surg.* **2003**, *30*, 507.
- [6] O. E. Teebken, A. M. Pichlmaier, A. Haverich, *Eur. J. Vasc. Endovasc. Surg.* **2001**, *22*, 139.
- [7] M. Demura, T. Asakura, T. Kuroo, *Biosensors* **1989**, *4*, 361.
- [8] T. Asakura, D. L. Kaplan, *Encyclopedia of Agricultural Science*, (Ed.: C. J. Arutzen), **1994**, *4*, 1.
- [9] M. Demura, T. Asakura, *Biotechnol. Bioeng.* **1989**, *33*, 598.
- [10] M. Demura, T. Asakura, *J. Membrane Sci.* **1991**, *59*, 39.
- [11] C. Vepari, D. L. Kaplan, *Prog. Polym. Sci.* **2007**, *32*, 991.
- [12] H. J. Jin, J. Chen, V. Karageorgiou, G. H. Altman, D. L. Kaplan, *Biomaterials* **2004**, *25*, 1039.
- [13] X. Zhang, B. Cassandra, D. L. Kaplan, *Biomaterials* **2008**, *29*, 2217.
- [14] L. Meinel, S. Hofmann, V. Karageorgio, L. Zincher, R. Lager, D. L. Kaplan, G. Vunjak-Novakovic, *Biotechnol. Bioeng.* **2004**, *88*, 379.
- [15] L. Soffer, X. Wang, Z. Xiaohui, J. Kluge, L. Dorfmann, D. L. Kaplan, G. Leisk, *J. Biomater. Sci. - Polym. Ed.* **2008**, *19*, 653.
- [16] D. N. Rockwood, E. S. Gil, S. Park, J. A. Kluge, W. Grayson, S. Bhumiratana, R. Rajkhowa, X. Wang, S. J. Kim, G. Vunjak-Novakovic, D. L. Kaplan, *Acta Biomater.* **2011**, *7*, 144.
- [17] J. R. Mauney, S. Sjostorm, J. Blumberg, R. Horan, J. P. O'Leary, G. Vunjak-Novakovic, V. Volloch, D. L. Kaplan, *Calcified Tissue Int.* **2004**, *74*, 458.
- [18] C. Li, C. Vepari, H. Jin, H. Kim, D. L. Kaplan, *Biomaterials* **2006**, *27*, 3115.
- [19] M. Lovett, E. George, J. A. Kluge, C. Cannizzaro, G. Vunjak-Novakovic, D. L. Kaplan, *Organogenesis* **2010**, *6*, 217.
- [20] S. Enomoto, M. Sumi, K. Kajimoto, Y. Nakazawa, R. Takahashi, C. Takabayashi, T. Asakura, M. Sata, *J. Vasc. Surg.* **2010**, *51*, 155.
- [21] T. Yagi, M. Sato, Y. Nakazawa, K. Tanaka, M. Sata, K. Itoh, Y. Takagi, T. Asakura, *J. Artif. Organs* **2011**, *14*, 89.
- [22] S. Min, X. Gao, L. Liu, *J. Biomater. Sci. - Polym. Ed.* **2009**, *20*, 1961.
- [23] D. Weiss, K. J. Wardrop, *Scalm's Veterinary Hematology*, 6th edition, Wiley-Blackwell **2006**.
- [24] S. Ravi, Z. Qu, E. L. Chaikof, *Vascular* **2009**, *17*, 45.
- [25] K. Hayashi, H. Handa, S. Nagasawa, A. Okumura, K. Moritake, *J. Biomech.* **1980**, *13*, 175.
- [26] H. Sonoda, S. Urayama, K. Takamizawa, Y. Nakayama, C. Uyama, H. Yasui, T. Matsuda, *J. Biomed. Mater. Res.* **2002**, *60*, 191.